

Climate-driven thresholds in reactive mineral retention of soil carbon at the global scale

Marc G. Kramer^{1*} and Oliver A. Chadwick²

Soil organic matter can release carbon dioxide to the atmosphere as the climate warms. Organic matter sorbed to reactive (iron- and aluminium-bearing) soil minerals is an important mechanism for long-term carbon storage. However, the global distribution of mineral-stored carbon across climate zones and consequently its overall contribution to the global soil carbon pool is poorly known. We measured carbon held by reactive minerals across a broad range of climates. Carbon retained by reactive minerals was found to contribute between 3 and 72% of organic carbon found in mineral soil, depending on mean annual precipitation and potential evapotranspiration. Globally, we estimate ~600 Gt of soil carbon is retained by reactive minerals, with most occurring in wet forested biomes. For many biomes, the fraction of organic carbon retained by reactive minerals is responsive to slight shifts in effective moisture, suggesting high sensitivity to future changes in climate.

Soils form by incongruent weathering of rock minerals, the incorporation of degraded organic matter and the subsequent reorganization of their chemical constituents. Fundamental to C storage in soil is the production of soluble organic compounds during microbial decomposition of organic matter and its stabilization via ligand exchange reactions with hydroxyl groups on the surfaces of newly formed mineral colloids^{1,2}. Even small amounts of these Fe- and Al-bearing reactive mineral colloids provide an important substrate for storing organic compounds. Dissolved organic carbon (DOC) retained by mineral colloids is known to be an important mechanism for long-term C accumulation in mineral soil^{2–9}. Because climate controls the rates of mineral weathering and the types of metal–silicate colloids produced, as well as the nature of organic compounds produced by plants, there is considerable variation in the production rates of soluble organic matter and its stabilization mechanisms within Earth's soils.

Although climate is an important factor in soil formation¹⁰, its role in regulating both the supply of DOC and the concomitant formation of reactive minerals to store that C has not been evaluated on a global scale. Local studies show that shifts in soil water balance cause nonlinear changes in many soil properties, including pH, nutrient supply^{11–14} as well as biological properties^{15,16} that are likely to be important in determining the amount and type of C storage¹⁷. At a global scale, climate determines a strong pH shift from 8 to 5 over a relatively narrow range of effective moisture¹⁸. Although this range in soil pH implies large differences in soil chemical processes and the mechanisms governing C stabilization¹⁹, we have little understanding of how 'effective moisture' influences soil C sorption by reactive minerals in broadly varying biomes.

Here, we consider how differences in effective soil moisture (precipitation after subtracting potential evapotranspiration (PET), assuming no overland redistribution of water) influence the amount of soil C retained by reactive minerals—defined here as the C released after chemical destruction of Fe- and Al-bearing mineral colloid co-precipitates using pyrophosphate-dithionite^{20,21}. We assembled a set of soil samples from the US National Science Foundation National Ecological Observatory Network (NEON) with additions from a globally distributed data set that represents

an annual rainfall range of about 100–4,100 mm (Fig. 1). For each soil, we quantified total organic and inorganic C and the fraction of C retained by reactive minerals.

Climate-driven thresholds of carbon retention

DOC released after reactive mineral dissolution contributed between 3 and 72% of total organic soil C, depending on mean annual precipitation (MAP) and PET (Fig. 2). At low MAP and high PET, annual effective moisture is in deficit (–1,200 to –300 mm MAP–PET), C retained by reactive minerals contributed little to total soil organic C (<6%) and changed very little with lower effective moisture (Fig. 2). By contrast, inorganic C content in Ca-bearing minerals (calcium carbonate) was greatest in the drier (–1,200 mm MAP–PET) sites and declined to zero where precipitation and evaporative losses are nearly balanced (Supplementary Fig. 2). A threshold, or rapid linear increase, in the amount organic C sorbed by reactive minerals (increasing from 6 to 62%) occurred at an effective moisture from –300 to 800 mm MAP–PET ($n=40$, $P<0.01$, $R^2=0.78$). Above 800 mm MAP–PET effective moisture, C sorbed by reactive mineral retention was the dominant constituent of subsoil C. Carbon retained by reactive minerals changed little with increasing precipitation above 800 mm MAP–PET effective moisture (63% on average), probably because the soils have reached their maximum C sorption capacity. Overall, we found that although effective moisture is a relatively weak predictor of total organic C content (Fig. 3), it exerts strong control on the fraction of organic C retained by reactive minerals across diverse parent materials and biomes (Fig. 2).

Many soil properties do not change linearly in response to extrinsic changes in soil-forming factors such as precipitation; instead their response is governed by 'pedogenic thresholds' that lead to nonlinear but predictable changes in soil properties and processes^{11,20}. Pedogenic thresholds represent a limit of soil property stability that can be exceeded by an intrinsic change in soil morphology, chemistry or mineralogy or by a gradual but progressive change in one of the external soil-forming factors^{11,20}. Our results show that thresholds in organic C retained by reactive minerals are also driven by differences in water flux (or effective moisture), probably due to nonlinear differences in the production and delivery

¹School of the Environment, Washington State University, Vancouver, WA, USA. ²Department of Geography, University of California, Santa Barbara, CA, USA. *e-mail: marc.kramer@wsu.edu

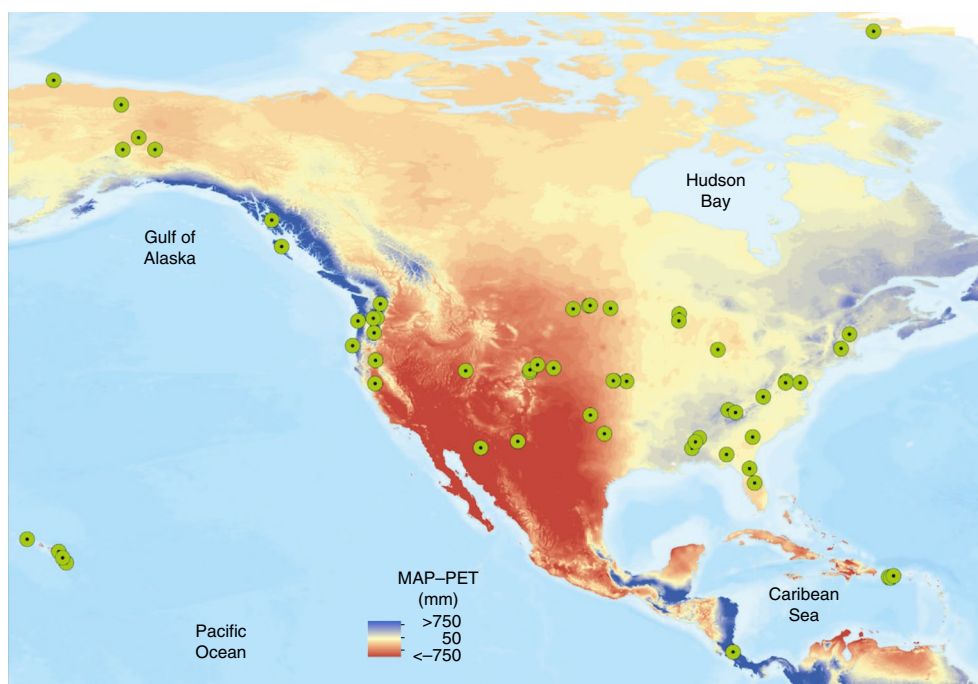


Fig. 1 | Effective moisture (mean annual precipitation after correcting for PET) and soil pit locations for NEON sites and a global archived data set over North and Central America. Other samples (not shown) used were from New Caledonia, Indonesia, Europe and Brazil (Supplementary Fig. 1).

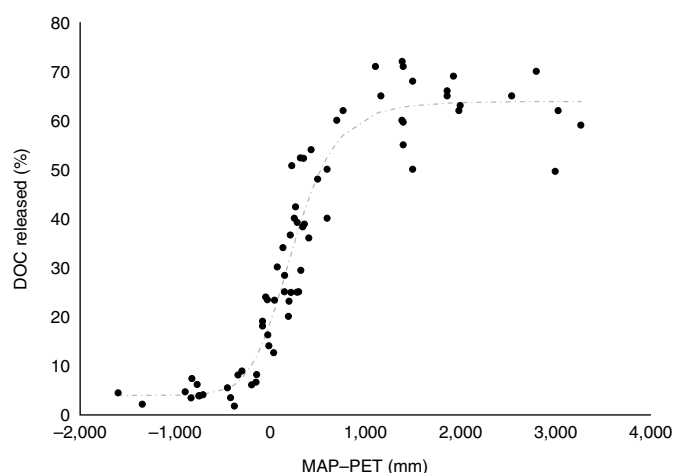


Fig. 2 | Percentage of organic carbon released as DOC after reactive mineral dissolution with pyrophosphate dithionite as a function of MAP adjusted for PET. PET was calculated using the Penman-Monteith method⁴¹. Depth integrated mineral horizon (B and C horizon) soil samples were from the National Ecological Observatory Network (NEON) and from a global soil data set (67 individual sites in total). The dashed line shows a nonlinear, symmetric sigmoidal fit: $y = 63.85736 + (3.886511 - 63.85736) / (1 + ((x + 1602) / 1839.642)^{8.060139})^{40}$.

of DOC as well as the formation of reactive minerals through weathering reactions, which are favoured under a wetter climate^{2,17}.

Soil chemical properties vary systematically across the range of climates and biomes represented in our data set¹⁸. At low precipitation and leaching potential, plant productivity is limited, there is little organic matter added to soil and there is little production of DOC. At neutral to alkaline pH, associated with arid and semi-arid soils, the solubility of Fe and Al is low, thereby limiting the opportunity for Al and Fe^{21,22} co-precipitation with organic matter²³. In these systems, calcium is likely to facilitate organic matter polymerization and

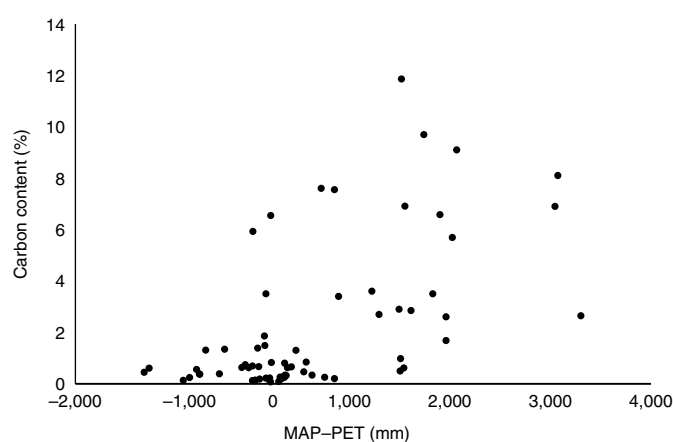


Fig. 3 | Relationship between total organic C content and MAP adjusted for PET. Depth integrated mineral horizon (B and C horizon) soil samples were from the National Ecological Observatory Network and a global soil data set (67 individual sites in total).

flocculation, which, combined with low water flux, limits the production and movement of DOC and its potential to associate with reactive mineral particles²³. At high precipitation (>800 mm MAP-PET) the throughflux of water and DOC saturate the system. Thick organic horizons (4–20 cm in our samples) are a characteristic feature of these wet soils, which support high production and movement of DOC into mineral soil horizons. Soluble soil constituents (for example, Ca, Mg, Si) are leached, and soil pH has been driven down by high levels of organic matter accumulation. Under low pH conditions DOC can sorb Fe and Al from solution or can be sorbed to larger mineral colloids by inner-sphere complexation reactions possibly facilitated by Ca via cation bridging^{21,22}. In either case, these reactive inorganic components retain large amounts of soil organic matter in the subsoil.

At an intermediate range of effective moisture (–300 to 800 mm MAP-PET), the system is highly responsive to changes in the

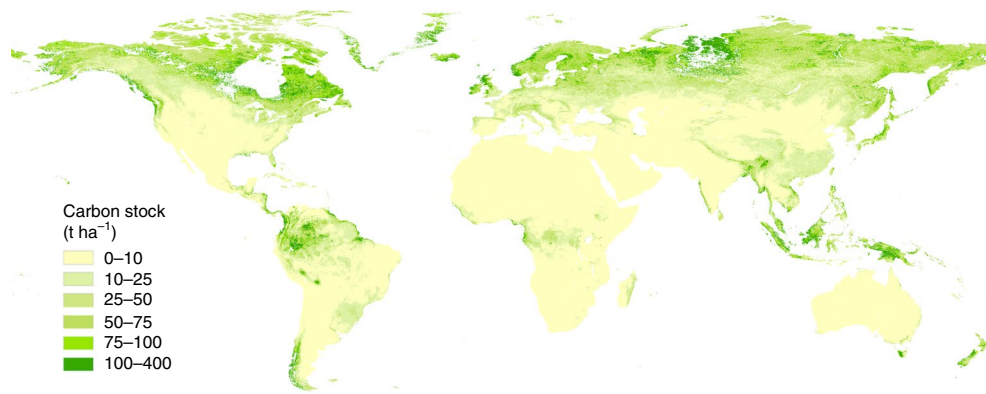


Fig. 4 | Global carbon stock of C retained by reactive minerals. Combining a spatially continuous global precipitation and PET data set^{24,25} with global soil C stock maps integrated by depth^{26,27} (all at 1 km resolution) and the relationships we observed, we calculated the contribution of C retained by reactive minerals to the total organic soil C pool.

magnitude of water moving through the system. With increased throughflux of water the amount of C retained by reactive minerals increased linearly from 6% to 62%. This linear increase represents a shift from calcium carbonate-dominated processes at low water throughput (Supplementary Fig. 2) to Fe- and Al-dominated C stabilization processes in soils that are strongly leached (Fig. 2)²³, which highlights the role of water as a mediator of both plant productivity and mineral weathering. Greater effective moisture leads to greater plant productivity and therefore more biologically produced acidity. The acidity is partly neutralized by rock weathering, which produces colloids that in turn sorb soluble organic C compounds. At lower precipitation Ca acts to flocculate DOC before it comes in contact with metals or colloids, whereas at higher precipitation, although Ca may still be involved^{21–23}, Al and Fe colloids interact to stabilize organic matter, typically at considerably lower concentrations. Hence, at high precipitation there is both more DOC and a greater flux of soil water available to move C deeper into soil profiles, bringing the solutions into contact with a greater volume of mineral colloids so that they can saturate the sorption capacity.

Soil carbon retention across biomes

Using the climate–mineral C relationship shown in Fig. 2, we estimated the contribution of C retained by reactive minerals to the global stock of soil C (Fig. 4). We combined spatially continuous global precipitation and PET data sets^{24,25} with global soil C stock maps integrated by depth^{26,27} (all at 1 km resolution), with our pyrophosphate-dithionite extract data to produce Fig. 4. Using this combined approach, we estimate that, globally, ~600 Gt C is retained by reactive minerals, which is approximately one-quarter of the total soil organic C pool (Figs. 4 and 5). In the high precipitation environments associated with forested biomes, reactive soil minerals retained the majority (>50%) of total organic soil C (Fig. 5). These results are in accord with other studies that used C sorption capacity calculations to show that up to 50% of the C in the subsoil was derived from DOC sorbed to mineral colloids⁷.

Our results quantify the role of precipitation-driven changes in C storage by reactive minerals in the subsoil and indicate that it is a major accumulation pathway in the global soil C pool for many biomes on Earth. Nearly one-third to one-half of the estimated 600 Pg of C associated with reactive soil minerals and total soil C stock is from biomes that are poorly represented in global soils data (for example, high latitudes) (Fig. 5), which points to the need for more data from these regions²⁸.

It is evident that there are strong correlations between climate and C retention by reactive minerals in soils (Fig. 2). We explored the spatial variability by classifying the land surface into Holdridge

	Holdridge life zone	Total C stock (Gt)	Reactive mineral C stock (Gt)	Reactive mineral C percent of total (%)	Penman–Monteith MAP–PET (mm)	
Desert	Tropical desert	2.6	0.2	6.3	-2,594	
	Tropical desert bush	1.5	0.1	6.4	-2,341	
	Subtropical desert	6.2	0.4	6.4	-2,195	
	Tropical thorn steppe	3.7	0.3	6.9	-2,051	
	Subtropical desert bush	8.9	0.6	6.8	-1,927	
	Warm temperate desert	1.4	0.1	6.4	-1,598	
	Warm temperate desert bush	5.2	0.3	6.6	-1,457	
	Subtropical thorn steppe	9.1	0.6	7	-1,447	
	Tropical very dry forest	8.4	0.6	7.4	-1,299	
	Cool temperate desert	15.2	1	6.5	-1,174	
Dry forest	Warm temperate thorn steppe	8.1	0.5	6.6	-1,109	
	Cool temperate desert bush	29	2	6.8	-937	
	Subtropical dry forest	35.6	3.7	10.4	-705	
	Boreal desert	9	1.5	16.4	-548	
	Warm temperate dry forest	18.5	2.3	12.4	-533	
	Cool temperate steppe	97.7	10.3	10.5	-509	
	Boreal dry bush	60.6	9.3	15.3	-398	
	Tropical dry forest	39.3	9.3	23.7	-258	
	Polar dry tundra	20.7	3.9	19	-222	
	Polar desert	276.5	53.3	19.3	-107	
Tundra	Polar moist tundra	142.5	28.3	19.9	-55	
	Boreal moist forest	579.5	109.9	19	19	
	Cool temperate moist forest	169.4	42.9	25.3	73	
	Polar wet tundra	238.2	55.5	23.3	93	
	Subtropical moist forest	120.7	37.2	30.8	269	
	Boreal wet forest	277	67.8	24.5	318	
	Warm temperate moist forest	22	7.8	35.4	328	
	Polar rain tundra	57.2	21.3	37.3	380	
	Cool temperate wet forest	25.6	12	46.7	497	
	Boreal rain forest	18.1	8.3	45.5	640	
Moist forest	Cool temperate rain forest	5.8	2.9	49.8	926	
	Tropical moist forest	108.2	51	47.1	1,046	
	Warm temperate wet forest	3.2	1.9	57.9	1,147	
	Subtropical wet forest	62.7	34.4	54.8	1,437	
	Warm temperate rain forest	1	0.6	64.1	1,892	
	Tropical wet forest	5.1	3	58.3	2,018	
	Subtropical rain forest	3.7	2.3	62.6	2,902	
	Wet forest					
	All biomes		2497.2	587.2		

Fig. 5 | Total and reactive mineral soil C stock by biome. Calculated C stock retained by reactive minerals by biome is based on Fig. 2 (for details see Methods). The percentage of the total C sorbed by reactive minerals is calculated as reactive mineral C stock/ total stock × 100) for biomes globally. MAP after adjusting for PET for each biome was calculated from 1 km grid cell values averaged over the entire biome.

life zones, which is a classification scheme based on the relationship between potential vegetation cover and climatic variables^{29–31}. The fraction of organic C retained by reactive minerals varied by Holdridge life zone (and precipitation amount after correcting for PET) (Figs. 5 and 6). Reactive minerals in wet forest ecosystem retained the greatest fraction organic C. By contrast desert biomes contained only a small fraction of the total organic soil C retained by reactive minerals (Figs. 5 and 6).

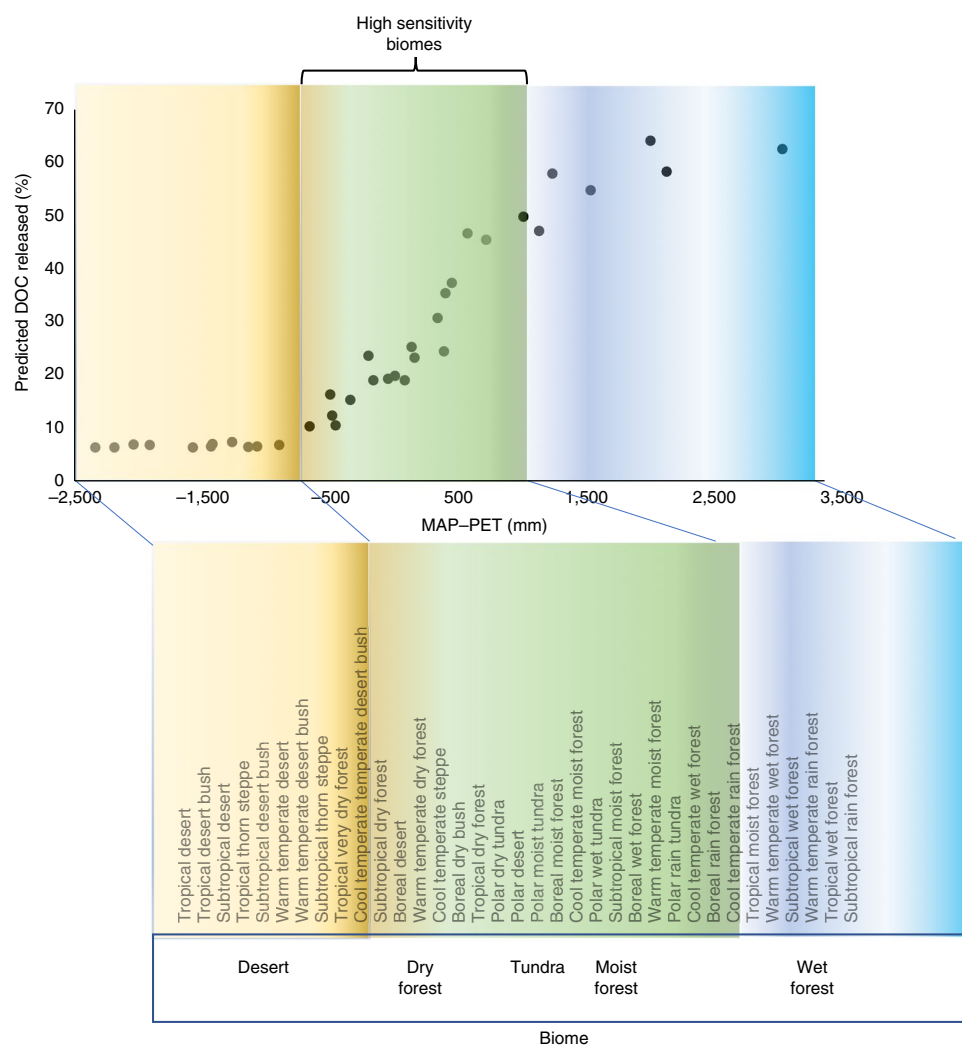


Fig. 6 | Predicted percentage of organic carbon released as DOC by reactive minerals by biome as predicted by effective moisture (MAP-PET).

Climate and soil C accumulation

Climate exerts first-order control on C transport and reactive mineral formation across diverse mineralogies and parent material, topographic conditions, vegetation and age of substrates¹⁰. Our results suggest that water-driven changes in soil properties exert strong control over the percentage of C stored by reactive minerals (Fig. 2). However, there was also variation (50–72%) across the wetter (MAP-PET > 800 mm) sites. Some of the lower values (between 50 and 63%) found at high rainfall sites occurred on younger geologic substrates (for example, post glacial landscapes < 20 kyr) indicated that weathering may not have advanced sufficiently for metastable reactive mineral accumulation. By contrast, higher values (up to 72%) were found on older surfaces, such as those found in Hawaii (20–4,100 kyr), indicating that weathering coupled with DOC production and delivery has advanced sufficiently to favour C retention by reactive minerals². Total organic C content varies less systematically with climate (Fig. 3) than the percentage of organic C retained by reactive minerals (Fig. 2), suggesting that interactions between climate and other controls on soil development (for example, mineralogy, vegetation, topography and time) also exert strong control on organic C content.

Our results show that this climate-driven pathway of C accumulation results in distinct thresholds in the amount of C retained by reactive minerals in soil, related primarily to temperature, precipitation timing and magnitude and soil PET rates, all of which are expected to change significantly over the next 100 years as the Earth's

temperature warms³². In the most climatically responsive range of effective moisture (−300 to 800 mm MAP-PET), the system is highly responsive to changes in the flux of water moving through the system, and consequently most sensitive to changing future climates. Depending on water flux, the amount of C retained by reactive minerals across biomes can range from 6% up to 60% (Fig. 6). Wetter forested biomes (> 800 mm MAP-PET), may be less sensitive to gradual or more incremental climate change, because the system is saturated with C and water, and consequently may buffer changes in climate (Figs. 5 and 6). Similarly, in drier climates (< −300 mm MAP-PET), water is severely limiting and little change in the fraction of C retained by reactive minerals occurs across a wide range of effective moisture conditions. Consequently, changes in rainfall or warming temperatures within the dry zone may have minimal effects on organic C sorption to Fe and Al reactive mineral surfaces (Figs. 5 and 6), but may have significant impact on other C stabilization mechanisms such as the accumulation of carbonates (Supplementary Fig. 2)²³.

Our work identifies a climatically sensitive pathway for soil C accumulation with reactive minerals in the subsoil and quantifies its contribution to the soil C pool for major biomes of the world²⁹. It is likely that C that has accumulated via this mechanism in the subsoil persists over the long term³³ due to the ligand bonds that form between hydroxylated mineral surface carboxyl and phenolic functional groups in the dissolved organic matter². Carbon retained by reactive minerals in surface mineral soils (0–30 cm) is

characteristically younger than subsoil C pools^{2,34}. It may not be as persistent, due to increased microbial activity, destabilization of the mineral matrix as a result of fluctuating wetting (reducing) and drying (oxidizing) conditions³⁵, and other disruptive soil disturbance processes^{28,35}.

The relative importance of this pathway is largely dependent on soil water flux and associated inputs of DOC into the subsoil in conjunction with the formation of reactive minerals. For many biomes on Earth, the fraction of organic C retained by reactive minerals is responsive to slight shifts in effective moisture, which suggests high sensitivity to future changes in climate (Figs 5 and 6). Models predicting future changes to climate and C dynamics should focus on incorporating DOC production, delivery and interaction with reactive minerals in the subsoil, in conjunction with substrate age and mineralogy, as this represents a significant (~24% total soil C) pathway for long-term C accumulation in the global soil C pool² and the dominant form of C accumulating in the subsoil for many biomes on Earth.

Online content

Any methods, additional references, Nature Research reporting summaries, source data, statements of data availability and associated accession codes are available at <https://doi.org/10.1038/s41558-018-0341-4>.

Received: 26 February 2018; Accepted: 19 October 2018;
Published online: 26 November 2018

References

- Gu, B., Schmitt, J., Chen, Z., Liang, L. & McCarthy, J. F. Adsorption and desorption of natural organic matter on iron oxide: mechanisms and models. *Environ. Sci. Technol.* **28**, 38–46 (1994).
- Kramer, M. G., Sanderman, J., Chadwick, O. A., Chorover, J. & Vitousek, P. M. Long-term carbon storage through retention of dissolved aromatic acids by reactive particles in soil. *Glob. Change Biol.* **18**, 2594–2605 (2012).
- Kaiser, K., Guggenberger, G. & Zech, W. Sorption of DOM and DOM fractions to forest soils. *Geoderma* **74**, 281–303 (1996).
- Kaiser, K. & Guggenberger, G. The role of DOM sorption to mineral surfaces in the preservation of organic matter in soils. *Org. Geochem.* **31**, 711–725 (2000).
- Guggenberger, G. & Kaiser, K. Dissolved organic matter in soil: challenging the paradigm of sorptive preservation. *Geoderma* **113**, 293–310 (2003).
- Jardine, P., McCarthy, J. & Weber, N. Mechanisms of dissolved organic carbon adsorption on soil. *Soil Sci. Soc. Am. J.* **53**, 1378–1385 (1989).
- Kalbitz, K. & Kaiser, K. Contribution of dissolved organic matter to carbon storage in forest mineral soils. *J. Plant Nutr. Soil Sci.* **171**, 52–60 (2008).
- Kalbitz, K., Schwesig, D., Rethemeyer, J. & Matzner, E. Stabilization of dissolved organic matter by sorption to the mineral soil. *Soil Biol. Biochem.* **37**, 1319–1331 (2005).
- Kalbitz, K., Solinger, S., Park, J.-H., Michalzik, B. & Matzner, E. Controls on the dynamics of dissolved organic matter in soils: a review. *Soil Sci.* **165**, 277–304 (2000).
- Jenny, H. *Factors of Soil Formation: A System of Quantitative Pedology* (Courier Corporation, New York, 1994).
- Chadwick, O. A. & Chorover, J. The chemistry of pedogenic thresholds. *Geoderma* **100**, 321–353 (2001).
- Dixon, J. L., Chadwick, O. A. & Vitousek, P. M. Climate-driven thresholds for chemical weathering in postglacial soils of New Zealand. *J. Geophys. Res.* **121**, 1619–1634 (2016).
- Vitousek, P., Dixon, J. L. & Chadwick, O. A. Parent material and pedogenic thresholds: observations and a simple model. *Biogeochemistry* **130**, 147–157 (2016).
- Dahlgren, R., Boettinger, J., Huntington, G. & Amundson, R. Soil development along an elevational transect in the western Sierra Nevada, California. *Geoderma* **78**, 207–236 (1997).
- Peay, K. G. et al. Convergence and contrast in the community structure of Bacteria, Fungi and Archaea along a tropical elevation-climate gradient. *FEMS Microbiol. Ecol.* **93**, 5 (2017).
- Von Sperber, C., Stallforth, R., Du Preez, C. & Amelung, W. Changes in soil phosphorus pools during prolonged arable cropping in semiarid grasslands. *Eur. J. Soil Sci.* **68**, 462–471 (2017).
- Kramer, M. G. & Chadwick, O. A. Controls on carbon storage and weathering in volcanic soils across a high-elevation climate gradient on Mauna Kea, Hawaii. *Ecology* **97**, 2384–2395 (2016).
- Slessarev, E. et al. Water balance creates a threshold in soil pH at the global scale. *Nature* **540**, 567–569 (2016).
- Rasmussen, C. et al. Beyond clay: towards an improved set of variables for predicting soil organic matter content. *Biogeochemistry* **137**, 297–306 (2018).
- Muhs, D. R. Intrinsic thresholds in soil systems. *Phys. Geogr.* **5**, 99–110 (1984).
- Sowers, T., Adhikari, D., Wang, J., Yang, Y. & Sparks, D. L. Spatial associations and chemical composition of organic carbon sequestered in Fe, Ca, and organic carbon ternary systems. *Environ. Sci. Technol.* **52**, 6936–6944 (2018).
- Sowers, T. D., Stuckey, J. W. & Sparks, D. L. The synergistic effect of calcium on organic carbon sequestration to ferrihydrite. *Geochem. Trans.* **19**, 4 (2018).
- Rowley, M. C., Grand, S. & Verrecchia, E. P. Calcium-mediated stabilisation of soil organic carbon. *Biogeochemistry* **137**, 27–49 (2018).
- Zomer, R. J. et al. *Trees and Water: Smallholder Agroforestry on Irrigated Lands in Northern India* Research Report No. 122 (IWMI, 2007).
- Zomer, R. J., Trabucco, A., Bossio, D. A. & Verchot, L. V. Climate change mitigation: a spatial analysis of global land suitability for clean development mechanism afforestation and reforestation. *Agric. Ecosyst. Environ.* **126**, 67–80 (2008).
- Hengl, T. et al. SoilGrids250m: global gridded soil information based on machine learning. *PLoS ONE* **12**, e0169748 (2017).
- Batjes, N. *Overview of Procedures and Standards in Use at ISRIC WDC—Soils* Report No. 2016/02 (ISRIC, 2016).
- Jackson, R. B. et al. The ecology of soil carbon: pools, vulnerabilities, and biotic and abiotic controls. *Annu. Rev. Ecol. Evol. System.* **48**, 419–445 (2017).
- Holdridge, L. R. Determination of world plant formations from simple climatic data. *Science* **105**, 367–368 (1947).
- Holdridge, L. R. *Life Zone Ecology* (Tropical Science Center, San Jose, 1967).
- Post, W. M., Emanuel, W. R., Zinke, P. J. & Stangenberger, A. G. Soil carbon pools and world life zones. *Nature* **298**, 156–159 (1982).
- IPCC *Climate Change 2013: The Physical Science Basis* (eds. Stocker, T. F. et al.) (Cambridge Univ. Press, 2013).
- Kögel-Knabner, I. et al. Organo-mineral associations in temperate soils: integrating biology, mineralogy, and organic matter chemistry. *J. Plant Nutr. Soil Sci.* **171**, 61–82 (2008).
- Trumbore, S. E., Chadwick, O. A. & Amundson, R. Rapid exchange between soil carbon and atmospheric carbon dioxide driven by temperature change. *Science* **272**, 393–396 (1996).
- Buettner, S. W., Kramer, M. G., Chadwick, O. A. & Thompson, A. Mobilization of colloidal carbon during iron reduction in basaltic soils. *Geoderma* **221**, 139–145 (2014).
- Harvard Dataverse* (Harvard Univ., 2018); <https://doi.org/10.7910/DVN/NGFY6A>
- McKeague, J. An evaluation of 0.1 M pyrophosphate and pyrophosphate-dithionite in comparison with oxalate as extractants of the accumulation products in podzols and some other soils. *Can. J. Soil Sci.* **47**, 95–99 (1967).
- Mehra, O. & Jackson, M. Iron oxide removal from soils and clays by a dithionite-citrate system buffered with sodium bicarbonate. *Clays Clay Miner.* **7**, 317–327 (1958).
- Franzmeier, D., Hajek, B. & Simonson, C. Use of amorphous material to identify spodic horizons. *Soil Sci. Soc. Am. J.* **29**, 737–743 (1965).
- Lalonde, K., Mucci, A., Ouellet, A. & Gélinas, Y. Preservation of organic matter in sediments promoted by iron. *Nature* **483**, 198–200 (2012).
- Walter, I. A. et al. ASCE's standardized reference evapotranspiration equation. In *Proc. Watershed Management and Operations Management 2000* (eds Flug, M., Frevert, D. & Watkins, D. W. Jr) 1–11 (American Society of Civil Engineering, 2000).

Acknowledgements

The authors thank R. Johnson, D. Andreasen and G. Kahl for assistance with soil analyses. Soil sample preparation and analyses were conducted at the Stable Isotope and Organic Geochemistry Laboratory at Washington State University, Vancouver. This work was, in part, financially supported by National Research Initiative grant no. 2007–35107–18429 and from the USDA National Institute of Food and Agriculture grant no. 2017–05483. Soil samples were provided by NEON, which is a programme sponsored by the National Science Foundation and operated under a cooperative agreement with Battelle Memorial Institute.

Author contributions

M.G.K. conceived of the study, designed and executed soil sample analyses, as well as global soil C and climate data set analyses. M.G.K. wrote the manuscript, to which both authors contributed substantial interpretation, discussion and text.

Additional information

Supplementary information is available for this paper at <https://doi.org/10.1038/s41558-018-0341-4>.

Reprints and permissions information is available at www.nature.com/reprints.

Correspondence and requests for materials should be addressed to M.G.K.

Publisher's note: Springer Nature remains neutral with regard to jurisdictional claims in published maps and institutional affiliations.

© The Author(s), under exclusive licence to Springer Nature Limited 2018

Methods

Soil sampling. We selected soil profiles along a continentally representative network of sites from NEON in addition to a globally representative archived data set. In total, we examined 703 soil samples from 67 sites that spanned a wide range of precipitation (~105–4,100 mm MAP) and parent materials (for example, quartz-dominated, volcanic ash, ultramafic and sedimentary lithologies). At all field sites, soils were sampled by depth (and by genetic soil horizon) down to weathered rock or to about 2 m in depth. Air-dried samples were sieved (2-mm mesh) to remove large organic and mineral particles. A 1-mm sieve was used to further pick out large organic particles including roots, bark and other identifiable plant parts².

Quantification of carbon retained by reactive minerals. Dithionite selectively removes reactive minerals of Fe and Al, including crystalline forms, allophane and ferrihydrite, and extracts crystalline hydrous oxides of Fe and Al, but not opal, crystalline aluminosilicate clay minerals or crystalline primary mineral silicates^{37–39}. Most commonly Fe, Al and Si in the supernatant are measured as an indicator of reactive mineral quantity. In this study, we quantified the amount of C released into solution after reactive mineral dissolution by using pyrophosphate-dithionite as an extractant^{19,20}, because we were interested in quantifying the entire pool of carbon retained by Al and Fe reactive minerals, which included contributions from short-range-ordered minerals and Fe-bearing crystalline secondary minerals. We used the same approach as in ref. ¹⁷, but used pyrophosphate-dithionite instead of hydroxylamine^{20,21,38}.

The amount of C retained by total reactive minerals in the mineral subsoil was quantified using pyrophosphate-dithionite extractant^{37,39} composed of 0.1 M sodium dithionite, 0.2 M sodium pyrophosphate decahydrate and 1:10 soils: solution. To prevent the hydrolysis of organic matter as well as its protonation and reabsorption onto soil particles in contact with the solution, we adjusted the pH using 5 N HCl until it was circumneutral (pH 7.5)^{38,40}. Pyrophosphate-dithionite extractable DOC released into solution was determined by measuring the DOC released into solution (TOC-VCSH analyser, Shimadzu) and then subtracting out any background dithionite-pyrophosphate C concentration (<0.5 ppm DOC on any given run). Carbon and reactive mineral dissolution in deionized water was used as a control.

Carbon analyses. The total C content of soils was measured with a coupled continuous-flow elemental analyser–isotope ratio mass spectrometer (EA-IRMS) system including a vario EL III EA (Elementar Analysen system) interfaced with an Isoprime isotope ratio mass spectrometer (IRMS). Dry samples (<2 mm) were ground finely with a zirconium mortar and pestle, and loaded into tin boats. One standard was run for every 10 samples, and two blanks and conditioning and calibration standards were included at the beginning and end of each run. Samples were run in duplicate and were always within the range of the standards. Analysis of internal standards indicated an analytical error of <2% for C. For samples that did not test positively for the presence of carbonates using 0.1 M HCl, organic C content equalled total C content.

For samples that tested positively for the presence of carbonates using 0.1 M HCl, inorganic C was removed by suspending in a 0.1 M HCl solution overnight on a shaker and corrected for any mass loss changes and organic C loss associated with evaporate dissolution. Organic C was then determined by running the sample through the EA analyser for C content, after removal of carbonates (and correcting for mass loss). Inorganic C content was calculated by subtracting the organic C content from total C. All samples were analysed at the Organic Geochemistry and Stable Isotope Facility at Washington State University, Vancouver.

Quantification of soil C stocks by Holdridge life zones. Soil samples were weighted by their depth interval in the 30–200 cm (B and C horizons) depth range for C content, and summed across the entire soil profile, resulting in a single

depth-weighted value being assigned for each soil profile for reactive mineral C and bulk C content. Combining a spatially continuous global precipitation and PET data set^{24,25,41–43} with global soil C stock maps integrated by depth^{26,27} (all at 1 km resolution) and the relationships we observed (Fig. 2) for mineral (30–200 cm) soil, we estimated the contribution of the C retained by reactive minerals to the total organic soil C pool by major biome type. We used the Penman–Monteith PET method for short clipped grass^{41,44}. To determine the percent of total C retained by reactive minerals the following procedure was followed. A value of 6% was assigned to values <–300 mm MAP–PET. Between –300 and 800 mm MAP–PET, a linear relationship was applied ($n=36$, $P<0.01$, $R^2=0.73$) to estimate the percentage of total C retained by reactive minerals (6–63%). A value of 63% was assigned to values above 800 mm MAP–PET.

For permafrost soils, due to the paucity of data in that portion of the globe and greater uncertainty due to the frozen conditions, a conservative maximum estimate of 20% total C was applied to permafrost regions that had in excess of 20% based on the MAP–PET relationship²⁸. For surface mineral horizons (0–30 cm) we used the relationship from Fig. 2, derived from deeper (30–200 cm) mineral soil horizons, but we applied a conservative value (maximum value of 20% of total C) to any grid cells in excess of 20% based on the MAP–PET relationship (Fig. 2) due to the higher organic C content found in near-surface (0–30 cm) mineral (A) soil horizons. We applied values of evapotranspiration⁴⁵ in lieu of PET in very cold (<3 °C MAT) climates as these areas retained more persistent (late season) snow cover. Area calculations were determined for grid cells represented in geographic coordinate space using Mercator projections to determine actual area. The total amount of soil C retained by reactive minerals was calculated by multiplying 1 km International Soil Reference and Information Centre total organic soil C stock maps (for each depth range) by the percentage of total C retained by reactive minerals and summing the total amount of soil C from 0 to 200 cm depth for each grid cell multiplied by its grid cell size (in ha). Global C stock was calculated by summing the total C stock for all grid cells globally. The C stock for total C and reactive C was also calculated by summing the cell values (weighted by area) for each of the Holdridge zone biomes (using a geographic information system coverage of the Holdridge life zones)³⁰.

Data availability

Open raster, vector and tabular data are posted on the Harvard Dataverse under a CC0 Public Domain Dedication licence that allows full and unrestricted global use of the data generated during this research while giving proper citation to the original author. These posted data allow for full replication, at the minimum mapping unit, of the results generated during this analysis. The data that support the findings of this study are available at <https://doi.org/10.7910/DVN/NGFY6A>³⁶. Correspondence and requests for materials should be made to M.G.K.

References

- Aschonitis, V., Demertzi, K., Papamichail, D., Colombani, N. & Mastrociccio, M. Revisiting the Priestley–Taylor method for the assessment of reference crop evapotranspiration in Italy. *J. Agrometeorol.* **20**, 5–18 (2015).
- Aschonitis, V. G. et al. High-resolution global grids of revised Priestley–Taylor and Hargreaves–Samani coefficients for assessing ASCE-standardized reference crop evapotranspiration and solar radiation. *Earth Syst. Sci. Data.* **9**, 615–638 (2017).
- Itenfisu, D., Elliott, R. L., Allen, R. G. & Walter, I. A. Comparison of reference evapotranspiration calculations as part of the ASCE standardization effort. *J. Irrig. Drain. Eng.* **129**, 440–448 (2003).
- Zhang, K. et al. Vegetation greening and climate change promote multidecadal rises of global land evapotranspiration. *Sci. Rep.* **5**, 15956 (2015).